NORSAR ROYAL NORWEGIAN COUNCIL FOR SCIENTIFIC AND INDUSTRIAL RESEARCH

Internal Report No. 4-74/75

A KIRNOS SEISMOGRAPH IN THE NORSAR SEISMIC ARRAY

by

A. Dahle

Kjeller, 28 February 1975

F08606-74-C-0049

A KIRNOS SEISMOGRAPH IN THE NORSAR SEISMIC ARRAY

by

A. Dahle

NTNF/NORSAR
Post Box 51
N-2007 Kjeller
NORWAY

28 February 1975

Internal Report No. 4-74/75

CONTENTS

SUMMARY

As a part of a Nordic project on detection seismology, a Kirnos vertical broadband instrument was installed at NORSAR subarray 04B and operated over a period of about nine months. The high level of microseismic activity around 6 sec period, probably generated by wind storms and sea waves in the coastal areas of Norway, imposes a serious limitation on the detectability. With a magnification of 1K, the 50% detectability level for body waves is around m_b (NORSAR) = 5.8. Magnitude measurements comparable to those made in Eastern European countries differ from those measured from seismograms written by narrow band instruments.

INTRODUCTION

The differences in earthquake magnitudes measured from wide band (Kirnos) seismographs, such as are widely installed in the USSR ("East") and narrow band seismographs used in "Western" installations have been discussed at great lengths in the Geneva test ban negotiations (CCD). Operation of Hall-Sears (U.S.A.) and Kirnos (U.S.S.R.) seismometers at the same site suggests itself as a useful experiment directed to clarifying the discrepancies between "Eastern" and "Western" body wave magnitudes. These discrepancies are commonly explained in terms of the effects of earthquake spectra combined with instrumental responses in such a way that broadband instruments are likely to give a better answer to the "true" magnitude (Husebye et al, 1974). Another interesting problem related to the so-called scaling of the seismic spectrum concerns whether the magnitude difference is strongly dependent on frequency. Although a joint operation of the two seismograph systems should provide results relevant to both these topics, it is to be expected, however, that noise disturbances seriously limit the detection capability of a broadband system, particularly when the installation is not well removed from a continental margin (e.g., Norway). Accordingly, the purpose of this study is primarily to establish the detectability of a Kirnos installation at NORSAR. Secondly, the magnitude problem will be treated by comparing results obtained with other relevant work.

The vertical Kirnos SVK-2 broadband seismograph at NORSAR was dismantled in the last part of September 1974 after about nine months of regular operation. From the beginning of January 1974 recording was continuous for 5 days each week, with some gaps caused by power breakdown, etc. The effective recording time was about 50-60% of total time installed. For preparation and installation, we refer to Pettersen (1973) and Pettersen and Larsen (1974). Notes on the operating performance and progress are given by Bungum (1974 a and b).

With very few exceptions, all Kirnos recorded events are well recorded by the NORSAR short period array and are thus relatively precisely located and reported in the NORSAR bulletin, which has been used as reference in this study. Depth effects are not accounted for in the present analysis due to lack of reliable estimates.

DETECTABILITY OF THE KIRNOS SVK-2 SEISMOGRAPH

During the period of operation (Jan-Sep 1974) the seismograms from the Kirnos instrumentation have been read in comparison with the NORSAR bulletin. On an average some twelve events have been identified every month, with more events detected in summer than in winter. Table 1 shows number of events identified on a monthly basis. The relatively few events recorded in April, July and September can be explained by relatively longer periods of non-operation.

Table 4 contains the comparison of NORSAR and Kirnos event parameters for the months January, February, August and September.

There is a predominance of later, longer period phases on the Kirnos recordings, and many of the seismograms show Rayleigh wave trains without any identifiable body wave phases. In fact, surface waves contaminating the recordings for hours is an outstanding feature seen on the Kirnos, and thus the probability of interference with and masking of other events is relatively high. However, the limitation on the average recording ability, i.e., detectability, is mainly caused by the noise level. Since the period range 3-8 secs, in which microseismic energy is generally intense, is included in the effective pass band of the Kirnos broadband response, (see Fig. 1) the detectability during noisy periods is indeed very poor.

Fig. 2a shows an event from Aleutians with NORSAR magnitude 5.7 recorded at a moderate winter noise level. In comparison Fig. 2b shows a summer situation with low noise level for an event with NORSAR magnitude 5.1 from the same region. High frequency signals are rare, the only recording of good quality obtained being a Novaya Zemlya explosion of 29 August which is illustrated in Fig. 2c. This event saturated the NORSAR system, so NORSAR magnitude is not available.

NOISE LEVEL CONSIDERATIONS

The Kirnos noise recordings show well-modulated packets of energy with relatively sharp and constant carrier frequency. The noise theory developed by Longuet-Higgins (1952) can therefore be applied. According to this author, the expectation of maximum amplitude $E(A_{max})$ divided by the root-mean-square value of the random noise (M) is given by the asymptotic expression

$$E(A_{max})/M = (\ln N)^{\frac{1}{2}} + \tfrac{1}{2}\gamma\ (\ln N)^{-\frac{1}{2}} + R \qquad (1)$$

where $\gamma = 0.57722$ is Eulers constant and R is a remainder which can be neglected. N is the number of peaks in the sample from which the maximum amplitude is selected.

In order to obtain an interpretation of the seasonal noise level variation, the following procedure was adopted. Maximum noise amplitude $2\ A_{max}$ (peak-peak) was read (if data were available) over a period of one hour centered at noon or midnight, GMT. The number of noise peaks within an hour depends on the average period of the noise, which in winter time seems to be around 6 sec, while the summer noise seems to have a period on average around 4 sec.

Replacing in (1) the expectancy by the statistical mean value, we obtain the mean-square noise level

$$M = \bar{A}_{max} / [(\ln N)^{\frac{1}{2}} + \tfrac{1}{2}\gamma (\ln N)^{-\frac{1}{2}}] \qquad (2)$$

Table 2 shows the readings of maximum amplitude for the two typical periods of the year mentioned previously. It is apparent from this table that the noise level increases sharply in mid-September; therefore, only readings up to 17 Sep have been included in the definition of a summer noise level situation. Letting N=600 for winter and N=900 for summer, we obtain (Table 3) that the noise level in summer is 15 dB below the winter level. This result agrees with NORSAR noise level studies performed by Bungum (personal communication).

For the Kirnos recordings the dominant periods of body waves will be in the same frequency range as the microseismic noise peaks (see Fig. 1), so that fluctuations in noise level determines the fluctuations in seismic event detectability threshold. The increase dN in number of events N detected corresponding to a relative gain in SNR of dm_b body wave magnitudes is obtained from the frequency-magnitude relationship.

$$\log (1 + dN/N) = b \cdot dm_b \qquad (3)$$

The 15 dB decrease given in Table 3 is equivalent to $dm_b = -0.75$. Also, Table 3 gives the ratio

$$\frac{N+dN}{N} = 19/7$$

An estimate of b is then obtained using (3) which yields b = -0.58. Although one would expect that b should be much lower for a broadband system than for narrowband instruments, (Marshall et al, 1972), it must be emphasized that the results obtained here are tentative due to the limited amount of data available.

DETECTABILITY

The total number of events detected on the Kirnos during the period 1 Jan 1974 to 20 Sep 1974 is a few more than 100. Both surface and body wave detections are included in this number. In the corresponding time intervals NORSAR reported 2720 events. Some of the events detected by Kirnos were not reported (although detected) by NORSAR because they were local, and 4 of them saturated the NORSAR system so that no magnitude could be measured. The remaining ones, a total of 101 events, form the basic set for a detectability evaluation of the Kirnos installated at NORSAR subarray 04B. The method used for this purpose is a maximum likelihood estimation technique developed by Ringdal (1974), and is based on a set of binary decisions about whether or not the Kirnos system has detected NORSAR-reported events at various magnitudes.

Fig. 3 shows the decision histogram together with the maximum likelihood estimated thresholds of 5.7 and 6.4 for 50 and 90 per cent probability of detection, respectively. All wave modes are included in the detection decision in this case. When only body waves (P, PP, PcP, PKP) are considered, the results are even more modest for the Kirnos seismograph detectability, namely, 5.9 and 6.5 (see Fig. 4). However, it has to be pointed out that the reliability of the estimates decreases when sample size is significantly less than one hundred.

MAGNITUDE MEASUREMENTS AND COMPARISONS

Due to poor detectability, the Kirnos seismograph system would need years of operation in Norway in order to establish a reasonable data base suitable for statistical magnitude studies. However, it might be interesting to see if the limited data available follow the general trend that would be expected from a broadband instrument of the SVK-2 type. Due to the paucity of observations, no regionalization was attempted, and, moreover, core phases are excluded from the magnitude considerations in the following.

Magnitude calculations were performed according to the formula both for the Kirnos and Hall-Sears seismometer, namely:

$$m_b = \log_{10} \left(\frac{A}{T}\right) + Q(\Delta,h) \qquad (4)$$

where A is a zero-to-peak ground motion amplitude, T is the period and Q is the distance-depth correction for P-waves at depth h (Gutenberg and Richter, 1956). For computation of surface wave magnitude we used:

$$M_s = \log_{10} \left(\frac{A}{T}\right) + 1.66 \log_{10} (\Delta)$$

where A is peak-to-peak ground motion amplitude measured in nanometers around 20 sec period, T is the measured period and Δ is the epicentral distance in degrees.

Altogether 25 events in the distance range 18-91 degrees were jointly recorded as P-waves by the Kirnos and the NORSAR Hall-Sears instrument at subarray site 04B00, the two instruments being separated physically by only 2 meters. A comparison of the Hall-Sears narrowband channel response with the Kirnos response is shown in Fig. 1. The body wave magnitude m_b^E computed by the "Eastern" broadband instrument versus m_b^W computed by the "Western" SP instrument is shown in Fig. 5. According to Davies (1969), the difference

$m_b^E - m_b^W$ should be around 0.5 magnitude units, while Marshall et al (1972) found this relationship to be magnitude dependent, yielding

$$m_b^E = 1.12 m_b^W - 0.15 \qquad (6)$$

Both these curves are given in Fig. 5, and the data is not inconsistent with any of them.

The Hall-Sears m_b^W magnitudes are estimated roughly at 1 sec period, while the Kirnos magnitudes m_b^E are measured over a range of periods. This gives an opportunity to examine the difference $m_b^E - m_b^W$ as a function of period measured on the Kirnos, which is shown in Fig. 6. Although the data are scattered, a trend showing increasing difference with increasing period is quite clear.

Subarray 04B is ranked as an average site with respect to amplitude performance for most regions (Husebye et al, 1974). The single instrument magnitude previously denoted m_b^W can therefore be replaced by the NORSAR (beam) magnitude m_b^N without changing the overall picture represented by Figs. 5 and 6. This is demonstrated in Figs. 8 and 9. A slightly greater data set is now available since NORSAR magnitude can be measured even if the single instrument 04B00 is down. Note that the solid line of Fig. 8 is the 0.6 m_b difference line.

Also the (Rayleigh) surface wave magnitude has been calculated according to eq. (5) for a number of events. In cases where also the Kirnos body wave magnitude is available, m_b^E versus M_s^E has been plotted in Fig. 7. Fig. 7 also shows the relationship obtained by Bune et al (1969) for body wave magnitude versus surface wave magnitude for a Russian station. Note that Bune and his colleagues define the surface wave magnitude using the horizontal component of the surface waves.

DISCUSSION AND CONCLUSION

The results obtained in this study support the conclusion that the main cause of the discrepancy between "Eastern" and "Western" measurements of magnitude is the difference in frequency responses of the seismographs employed. A rough estimate of the slope b of the frequency-magnitude relationship for the Kirnos gives a much lower value than reported for "Western" narrowband instrumentation (Richter, 1958; Marshall et al, 1972). Thus by extrapolation, "Western" data predicts more small shocks and fewer great shocks than "Eastern" broadband data collected by Kirnos instruments. The Kirnos event detectability is poor, as the noise level imposes a serious limitation on this broadband system. In our view such a system is most useful for general seismological research purposes, but considered highly inadequate for monitoring of underground nuclear explosions. In conclusion, it should be stressed that in the present context a minimum requirement for a useful broadband seismograph system should include magnetic tape recording to permit such operations as frequency filtering.

REFERENCES

Bune, V.I., N.A. Vvedenskaya, I.V. Gorbunova, N.V. Kondorskaya, N.S. Landyreva and I.V. Fedorova (1970): Correlation of M_{LH} and m_{pv} by data of the network of seismic stations of the U.S.S.R., Geophys. J.R. Astr. Soc., 19, 533-542.

Bungum, H. (1974a): Semiannual Technical Summary, 1/7-31/12-1973, NORSAR Scientific Report No. 4-73/74, NTNF/NORSAR, Kjeller, Norway.

Bungum, H. (1974b): Semiannual Technical Summary, 1/1-30/6-1974, NORSAR Scientific Report No. 6-73/74, NTNF/NORSAR, Kjeller, Norway.

Davies, D. (1968): Seismic methods for monitoring underground explosions, Almquist & Wiksell, Sweden.

Gutenberg, B., and C.F. Richter (1956): Magnitude and energy of earthquakes, Ann. di Geophis., 9, 1-15.

Husebye, E.S., A. Dahle and K.A. Berteussen (1974): Bias analysis of NORSAR and ISC-reported seismic event magnitudes, J. Geophys. Res., 79, 20, 2967-2978.

Longuet-Higgins, M.S. (1952): On the statistical distribution of the heights of sea waves, J. of Marine Res., XI, No. 3.

Marshall, P.D., R.F. Burch and A. Douglas (1972): How and why to record broadband seismic signals, Nature, 239, No. 5368, 154-155.

Pettersen, R. (1973): Report from a visit related to the Kirnos project at NDPC, Internal Report No. 4-73/74, NTNF/NORSAR, Kjeller, Norway.

Pettersen, R., and P.W. Larsen (1974): Installation of Kirnos, Internal Report No. 7-73/74, NTNF/NORSAR, Kjeller, Norway.

Richter, C.F. (1958): Elementary Seismology, W.H. Freeman & Company, San Francisco and London.

Ringdal, F. (1974): Estimation of Seismic Detection Thresholds, Technical Report No. 2, Texas Instruments, P.O. Box 6015, Dallas, Texas, 75222, 28 May 1974.

ACKNOWLEDGEMENT

Contributions from the whole NORSAR staff during the progress of this study are greatly appreciated. In particular, A. Nilsen from Array Monitoring group and the employees at NORSAR Maintenance Center are thanked for their efforts.

We are also indebted to Professor H. Korhonen, University of Oulu, Finland, and Mr. Seppo Pirhonen, University of Helsinki, Finland, for their co-operation in the experiment.

Month	No. of Events	Surface Waves Only
January	7	5
February	7	2
March	13	9
April	5	2
May	22	3
June	18	3
July	9	2
August	23	7
September	7	4

Table 1

Number of events recorded on Kirnos during the period of operation Jan-Sep 1974.

DATE	NOISE AMPL. (P-P) 10^{-6}m		DATE	NOISE AMPL. (P-P) 10^{-6}m	
	Day	Night		Day	Night
02 Jan	5.0	4.8	02 Aug	0.6	0.5
03 Jan	6.5	8.5	05 Aug	0.3	0.3
08 Jan	3.2	3.5	06 Aug	0.3	0.3
09 Jan	4.5	3.8	07 Aug	0.3	0.3
10 Jan	2.6	4.8	08 Aug	0.3	0.3
11 Jan	9.0	5.5	09 Aug	0.5	0.9
15 Jan	6.0	2.7	12 Aug	0.4	0.3
17 Jan	3.0	3.6	13 Aug	0.5	0.5
18 Jan	4.0	7.5	15 Aug	0.4	0.5
22 Jan	9.0	8.5	16 Aug	0.4	0.7
24 Jan	4.2	4.3	19 Aug	0.3	0.4
25 Jan	2.0	1.7	22 Aug	1.0	0.5
29 Jan	6.0	5.5	23 Aug	1.5	1.0
30 Jan	5.5	5.2	26 Aug	1.5	2.0
31 Jan	6.3	6.0	27 Aug	1.8	1.1
01 Feb	5.0	6.5	28 Aug	1.6	0.6
04 Feb	5.0	1.8	29 Aug	0.8	0.7
05 Feb	1.5	3.5	30 Aug	0.7	0.5
06 Feb	3.2	3.4	02 Sep	0.5	0.5
07 Feb	1.4	2.3	04 Sep	1.0	0.8
08 Feb	3.0	4.0	03 Sep	0.5	1.3
11 Feb	5.7	6.3	05 Sep	0.8	1.0
12 Feb	7.5	6.5	06 Sep	1.0	2.0
13 Feb	5.0	4.7	09 Sep	4.7	2.8
14 Feb	3.3	4.5	10 Sep	2.5	-
15 Feb	5.3	7.5	11 Sep	1.0	1.4
20 Feb	6.0	2.0	12 Sep	2.0	2.0
21 Feb	2.5	2.8	13 Sep	0.5	0.5
22 Feb	7.0	10.5	16 Sep	0.3	0.4
25 Feb	3.7	5.8	17 Sep	2.0	4.5
26 Feb	4.3	2.5	18 Sep	7.0	9.5
27 Feb	2.4	3.0	19 Sep	6.0	6.0
28 Feb	4.0	5.5			
AVERAGE O-P	2.8×10^{-6}m		AVERAGE O-P (up to Sep 17)	0.5×10^{-6}m	
RMS NOISE	1.1×10^{-6}m		RMS NOISE	0.2×10^{-6}m	

Table 2

Microseismic activity expressed by measurement of maximum noise amplitude in one hour around mid-day or mid-night. RMS noise calculated by eq. (2).

Time of Year	Total Recording Time (hours)	Relative RMS Noise (dB)	No. of Body Waves Detected
Jan/Feb (winter)	785	0	7
Aug/Sep (summer)	772	- 15	19

Table 3

Body wave detections on Kirnos versus noise level variation.

NORSAR					KIRNOS SVK-2						
Arrival Time (P)	Region	Δ	T	M_b	Phase	Read at Time	A mm	T sec	M_s	M_b	Comments
10 Jan 09.10.21.6	New Hebrides Is.	130	1.4	6.4	PKP	09.10.20	6.5	7.0		6.9	
					LR	10.07.40	50.0	21.0	7.2		
22 Jan 13.38.38.1	Near East Coast Kamchatka	61	1.1	5.8	LR	14.06.20	4.5	19.0	5.6		Weak
24 Jan 19.24.01.8	Hokkaido, Japan	70	1.1	5.9	LR	19.54.50	33.0	18.0	6.5		
26 Jan 05.48.07.5	Off Coast of Jalisco, Mexico	88	1.2	4.9	LR	06.26.10	11.5	20.0	6.2		Quality 2
30 Jan 10.07.39.8	Aroe Is. Region	110	0.9	5.8	LR	11.03.12	11.0	20.0	6.4		
31 Jan 07.15.40.3	Kyushu, Japan	76	1.0	5.2	LR	07.52.28	18.5	16.0	6.3		
31 Jan 23.48.54.1	Solomon Isl.	121	1.2	5.7							Interfering Events
01 Feb 00.06.20.5	Greece-Bulg. Border	21	1.1	5.1							
01 Feb 03.31.22.0	Solomon Isl.	120	0.9	5.9							Interfering Events
03.46.54.1	-"-	"	0.8	5.1							
01 Feb 12.14.06.4	Southern Sumatra	95	1.0	5.4	LR	12.49.42	3.5	19.0	5.9		Weak
04 Feb 20.29.28.0	Solomon Isl.	121	0.9	5.5	LR	21.26.30	5.0	20.0	6.1		
06 Feb 04.14.54.2	Fox Is.,Aleutians	66	1.0	5.7	P	04.14.56	9.0	9.0		6.4	
					LR	04.44.44	19.0	20.0	6.3		
22 Feb 00.48.02.0	SE of Shikoku, Japan	78	0.9	6.0	P	00.48.05	3.0	6.0		6.0	Surface waves weak
28 Feb 14.19.15.5	Loyalty Is Region	140	1.3	5.3	PKP	14.19.35	6.0	6.0		6.4	Interfering Events
					LR	15.31.05	5.2	20.0	6.3		
28 Feb 20.32.39.1	Costa Rica	85	1.6	6.0	P	20.32.40	10.0	7.0		6.6	
					LR	21.09.00	11.5	20.0	6.2		

Table 4

List of parameters from the Kirnos detections compared to the NORSAR-solutions.
(Sheet 1 of 4)

NORSAR					KIRNOS SVK-2						
Arrival Time (P)	Region	Δ	T	M_b	Phase	Read at Time	A mm	T sec	M_s	M_b	Comments
06 Aug 18.57.41.6	Fiji Is Region	139	1.3	5.3	PKP	18.57.40	1.2	8.0		6.1	
					PP	19.00.40					
					LR	20.06.40	2.2	19.6	5.9		
07 Aug 08.33.55.3	Kodiak Is. Region	61	0.8	5.1	LR	09.01.30	1.0	18.0	4.9		Weak
08 Aug 01.28.09.8	Norwegian Sea	9	1.3	4.4	P	01.28.12	1.5	12.0		5.0	
					LR	01.32.40	8.5	19.0	4.8		
08 Aug 19.07.54.5	Norwegian Sea	9	1.3	4.2	LR	19.12.24	2.0	19.0	3.8		
08 Aug 19.28.44.7	Taiwan Region	78	0.8	5.1	P	19.28.50	1.5	10.4		5.6	
					LR	20.01.22	10.1	19.0	6.1		
08 Aug 23.27.37.4	Norwegian Sea	9	1.3	4.2	LR	23.32.24	1.8	18.8	3.8		
10 Aug 11.40.48.6	S. of Fiji Is.	140	1.0	5.8	PKP	11.40.42	0.7	4.0		6.2	No. LR wave
					SKS	11.47.50	1.5	4.4			deep?
13 Aug 03.57.12.7	Andreanof Is. Aleutians	69	1.0	5.4	P	03.57.16	3.5	8.8		6.0	
					PP	03.59.50					
					LR	04.24.55	10.5	22.0	6.1		
13 Aug 13.12.06.1	S. of Fiji Is.	142	1.5	5.4	PKP	13.12.06	0.6	3.6		6.1	
					LR	14.10.36	2.2	20.0	5.9		
14 Aug 05.45.46.5	Andreanof Is. Aleutians	67	1.1	5.2	P	05.45.46	1.4	7.0		5.7	
					LR	06.13.24	1.4	21.0	5.2		
					PP	05.48.29					
16 Aug 09.52.25.0	Andreanof Is. Aleutians	67	1.2	5.1	P	09.52.27	2.5	9.0		5.9	
					LR	10.20.04	5.4	22.0	5.8		
					PP	10.54.56					
17 Aug 05.23.08.7	Sea of Okhotsk	59	1.0	5.2	LR		1.6	15.0	5.0		

Table 4

(Sheet 2 of 4)

NORSAR					KIRNOS SVK-2						
Arrival Time (P)	Region	Δ	T	M_b	Phase	Read at Time	A mm	T sec	M_s	M_b	Comments
19 Aug 12.29.24.8	S. Coast of Honshu	76	0.9	5.3	LR	13.09.40	1.5	20.0	5.3		
19 Aug 20.07.10.0	Nicaragua	83	1.3	4.9	P	20.07.12	0.5	4.4		5.6	
23 Aug 04.10.49.3	Taiwan	79	1.1	4.6	LR	04.49.00	7.4	14.6	5.9		
23 Aug 05.08.49.8	Timor	110	0.9	5.6	PP	05.09.14	1.2	8.0		6.5	
					PKKP						
					LR	05.56.	2.4	16.7	5.7		
24 Aug 10.52.00.8	Fox Is.	68	0.9	5.7	P	10.52.00	2.7	5.8		6.1	
					LR	11.53.14	3.4	18.4	5.5		
27 Aug 13.04.00	S. Sinkiang				P	13.04.00	2.4	5.0		6.0	No. 20 sec LR wave
(Short Period					PP	13.05.45					
Analog Station)		45	0.9	6.0	PPP	13.06.18					
					PS	13.10.30					
					SS	13.13.40					
27 Aug 17.42.00.1	S. Sinkiang	44	0.8	5.0	LR	18.00.40	2.5	22.0	5.2		
29 Aug 03.09.50.2	S. of Fiji Is.	143	1.1	5.1	PKP	03.09.52	2.5	12.0		5.5	
29 Aug 10.04.35.6	Novaya Zemlya	21	0.7	-	P	10.04.36	13.5	3.0		6.4	Explosion
					S	10.08.18					
30 Aug 15.11.32.1	Calif.-Nevada border	74	1.1	5.6	P	15.11.34	0.5	2.0		5.9	
30 Aug 23.41.35.0	S. of Honshu	81	0.9	5.2	P	23.41.34	1.8	8.0		5.8	
					LR	00.20.00	4.7	18.0	5.8		

Table 4

(Sheet 3 of 4)

NORSAR					KIRNOS SVK-2						
Arrival Time (P)	Region	Δ	T	M_b	Phase	Read at Time	A mm	T sec	M_s	M_b	Comments
03 Sep 01.51.49.5	S. of Honshu	80	0.9	5.0	LR	02.30.50	2.5	18.0	5.6		
03 Sep 06.07.29.7	Philippine Is. Region	83	0.9	6.0	P	06.07.30	3.5	8.0		6.1	
					LR	06.46.48	14.0	16.0	6.5		
03 Sep 19.49.21.0	Kirgiz, SSR	42	0.9	5.4	LR	20.08.15	6.0	14.0	5.3		
04 Sep 06.18.34.5	S. of Java	100	1.0	5.3	i	06.40.30					No identifiable P-phase
					LR	06.49.00	12.0	19.0	6.4		
13 Sep 08.03.17.8	Near East Coast Kamchatka	62	1.1	5.9	P	08.03.16	1.5	9.0		5.6	Weak
					LR	08.33.30	2.5	20.0	5.4		
16 Sep 16.53.53.7	Kirgiz, SSR		1.0	5.0	LR						weak
17 Sep 05.15.18.2	Greece-Albania Border Region.	21	0.8	4.7	LR	05.24.48	5.5	14.0	4.8		

Table 4

(Sheet 4 of 4)

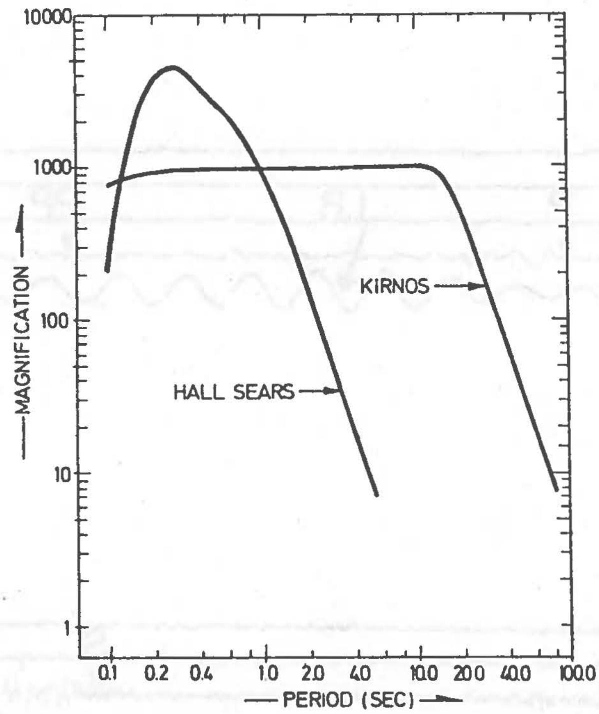

Fig. 1 Displacement response for Kirnos SVK-2 compared to the NORSAR seismometer response (Hall-Sears). Equal magnification at 1 sec period.

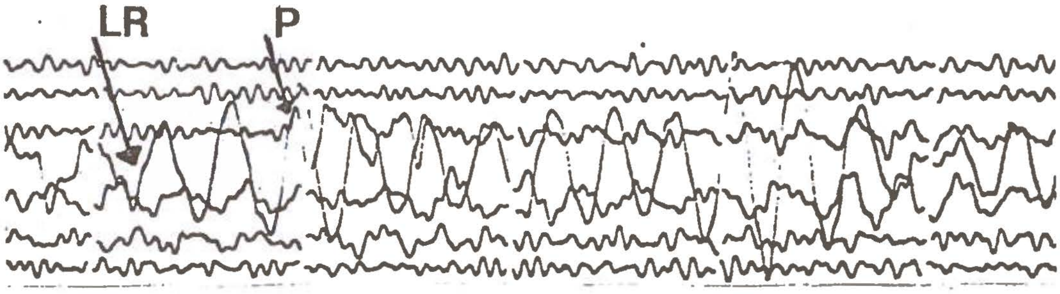

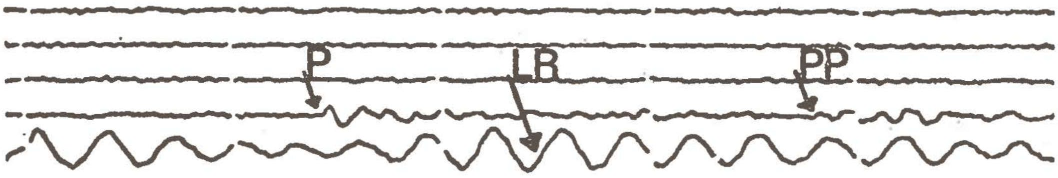

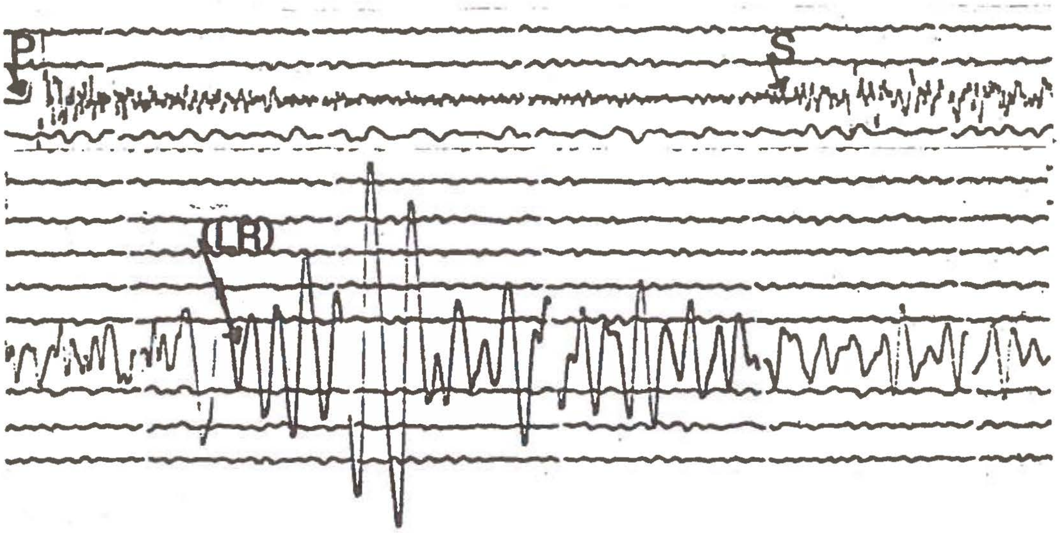

Fig. 2 a) Kirnos recording 06 Feb 04.14.54, Fox Islands, Aleutians. NORSAR m_b = 5.7

b) Kirnos recording 16 Aug 09.52.25, Andreanof Islands, Aleutians. NORSAR m_b = 5.1

c) Kirnos recording of Novaya Zemlya explosion 29 Aug 10.04.36. Kirnos m_b = 6.4

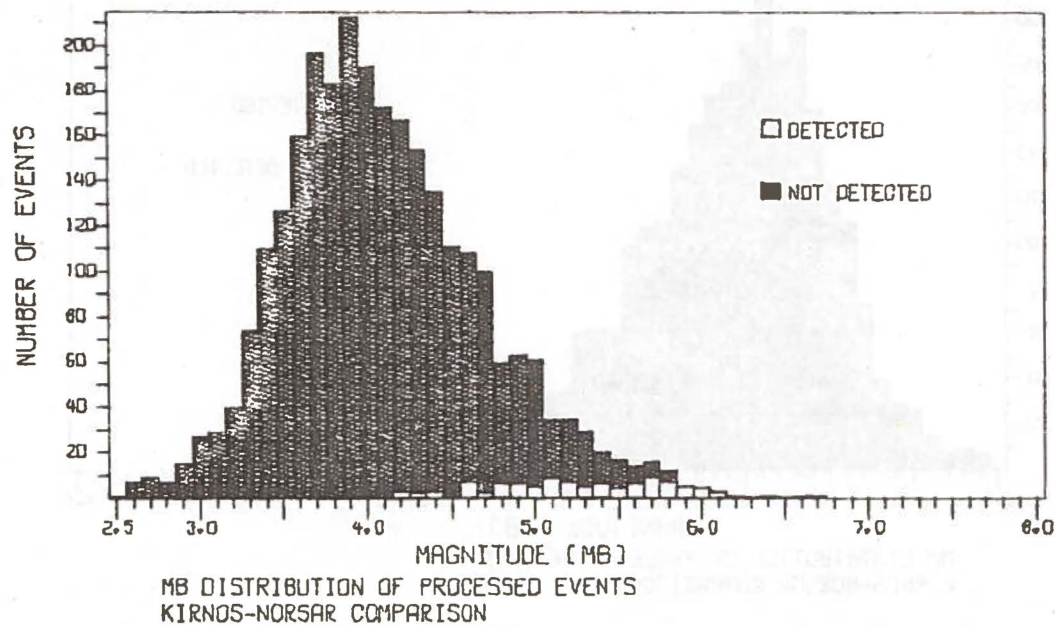

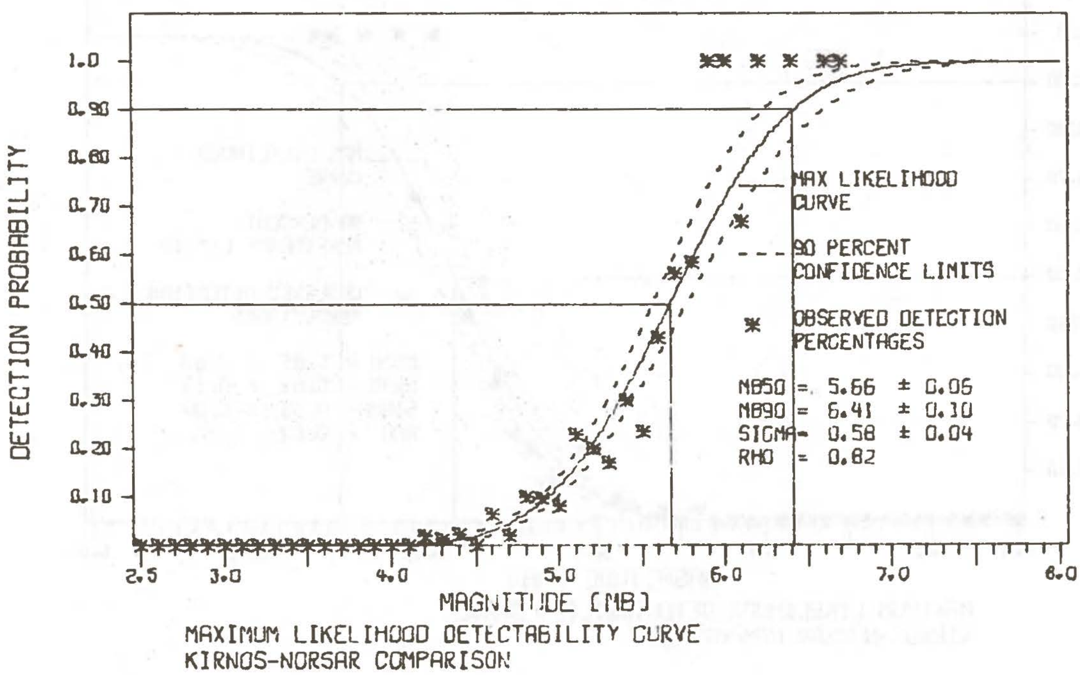

Fig. 3 Kirnos detection statistics for the total number of events identified (all phases included).

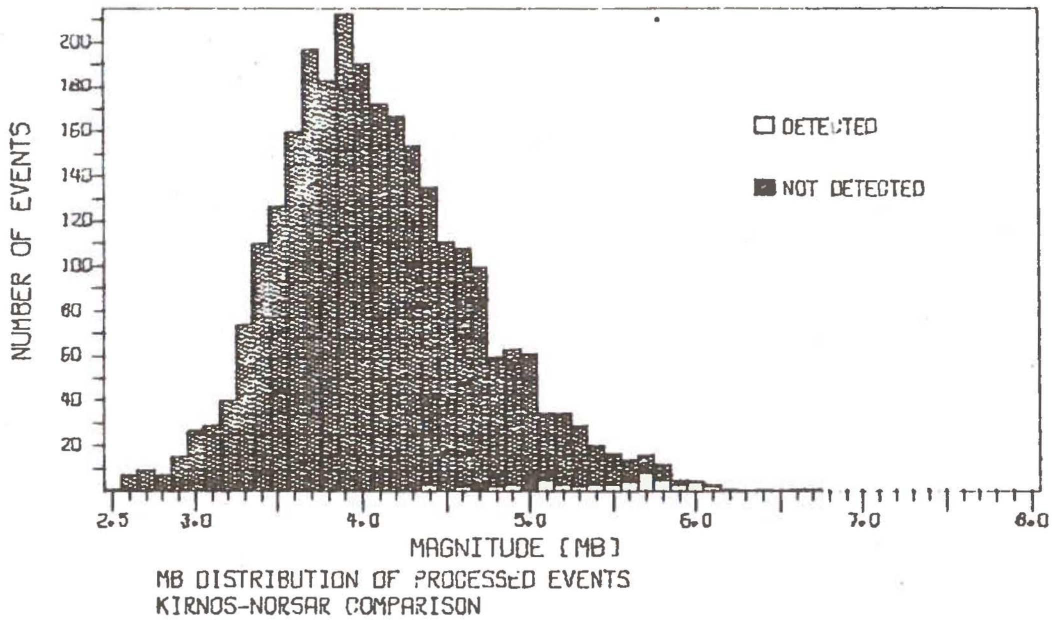

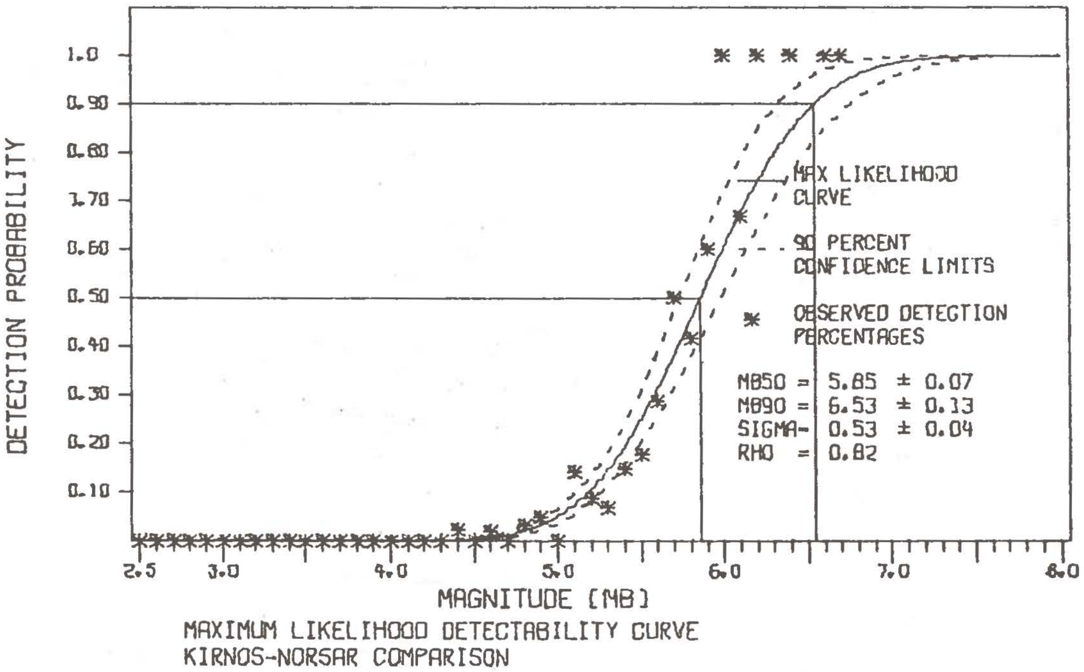

Fig. 4 Kirnos detection statistics for body wave phases identified.

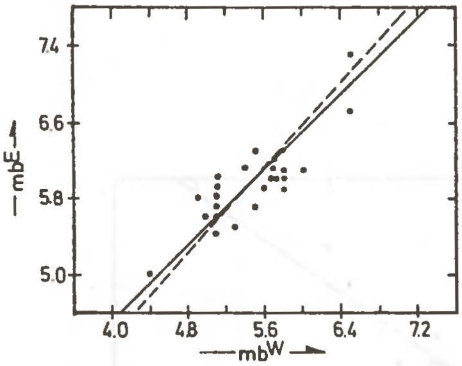

Fig. 5 Kirnos m_b^E versus Hall-Sears m_b^W. Dotted line: "Eastern" - "Western" magnitude relationship by Marshall et al (1972). Solid line: E-W magnitude relationship by Davies (1969).

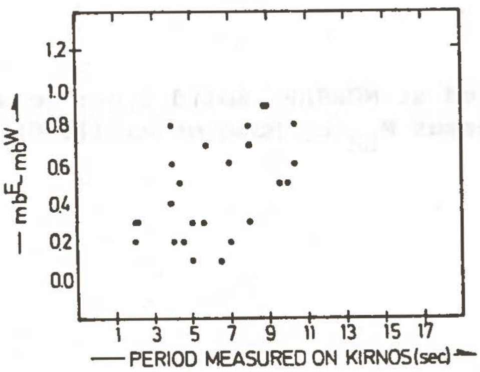

Fig. 6 Difference in magnitude m_b^E - m_b^W versus period measured on Kirnos recordings.

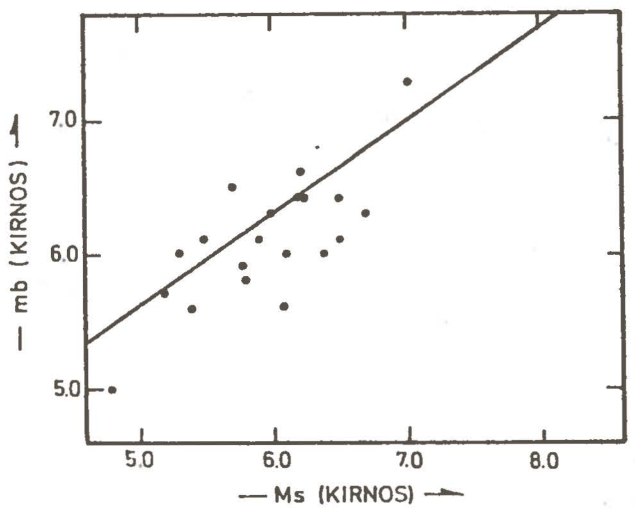

Fig. 7 m_b^E versus M_s^E measured at NORSAR. Solid line: relationship obtained for m_{pv} versus M_{LH} by Bune et al (1970) for Obninsk station.

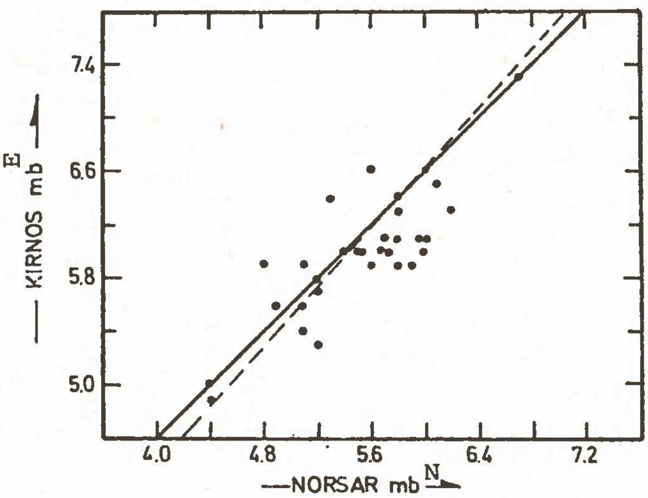

Fig. 8 Kirnos magnitude (m_b^E) versus NORSAR (beam) magnitude (m_b^N). Dotted line: "Eastern" - "Western" magnitude relationship by Marshall et al (1972). Solid line: 0.6 m_b difference line.

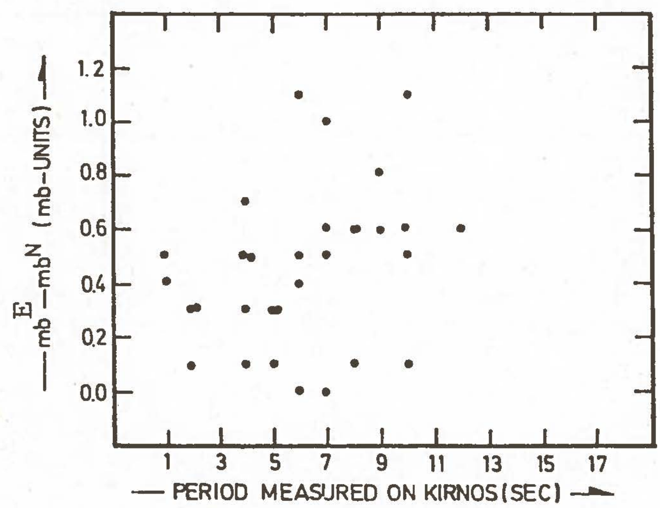

Fig. 9 Difference in Kirnos and NORSAR determined magnitude as a function of period measured on Kirnos.